THE ASTROPHYSICAL JOURNAL, 677: L31–L34, 2008 April 10

SECONDARY PHOTONS FROM HIGH-ENERGY PROTONS ACCELERATED IN HYPERNOVAE

KATSUAKI ASANO[1] AND PETER MÉSZÁROS[2,3,4]

Received 2008 January 28; accepted 2008 March 3; published 2008 March 18

ABSTRACT

Recent observations show that hypernovae may deposit some fraction of their kinetic energy in mildly relativistic ejecta. In the dissipation process of such ejecta in a stellar wind, cosmic-ray protons can be accelerated up to $\sim 10^{19}$ eV. We discuss the TeV to MeV gamma-ray and the X-ray photon signatures of cosmic rays accelerated in hypernovae. Secondary X-ray photons, emitted by electron-positron pairs produced via cascade processes due to high-energy protons, are the most promising targets for X-ray telescopes. Synchrotron photons emitted by protons can appear in the GeV band, requiring nearby (<40 Mpc) hypernovae for detection with *GLAST*. In addition, air Cerenkov telescopes may be able to detect regenerated TeV photons emitted by electron-positron pairs generated by CMB attenuation of π^0-decay photons.

Subject headings: cosmic rays — gamma rays: theory — radiation mechanisms: nonthermal — supernovae: general — X-rays: general

1. INTRODUCTION

Hypernovae (HNe) are a peculiar type of supernova with ejecta velocities and apparent isotropic-equivalent ejecta energies which are larger than usual, and with indications of anisotropy (Nomoto et al. 2008). Some of them are associated with long gamma-ray bursts (e.g., Woosley & Bloom 2006; a recent example being GRB 060218/SN 2006aj [e.g., Campana et al. 2006]), while others appear not to be. Cosmic rays up to energies $E \lesssim 10^{17}$ eV are thought to be accelerated in relatively normal supernova remnants (Hillas 2005). More recently, it has been suggested that HNe may accelerate cosmic-ray protons or nuclei up to energies $E \lesssim 4 \times 10^{18} Z$ eV (Wang et al. 2007, 2008; Budnik et al. 2008). The smoking-gun proof for cosmic-ray acceleration in supernova remnants would be the observation of very high energy ($\gtrsim$ TeV) neutrinos (e.g., Kistler & Beacom 2006), which will require completion of cubic kilometer detectors, or else the observation of secondary photons arising from pions, which remains inconclusive (e.g., Gabici & Aharonian 2007; Katz & Waxman 2008). Nonetheless, continued gamma-ray observation with air Cerenkov telescopes (ACTs) in the TeV range, and with *GLAST* and AGILE in the GeV range, may provide the best immediate hopes for resolving this question. In the present Letter, we consider the same question in relation to HNe, and address the question of the photons' signatures from secondaries arising from cosmic-ray acceleration in typical HNe.

In § 2 we describe our model NHs and consider the baryonic and photonic environment in which the explosion occurs, as well as its effect on the cosmic rays accelerated in the ejecta. In § 3 we discuss the Monte Carlo simulations performed on these models, and present the results for the photon signatures arising from various secondary components. In § 4 we discuss the detectability prospects for these signals, compared to the sensitivity of ACTs and *GLAST*, and summarize our results and conclusions.

[1] Interactive Research Center for Science, Tokyo Institute of Technology, 2-12-1 Ookayama, Meguro-ku, Tokyo 152-8550, Japan; asano@phys.titech.ac.jp.

[2] Department of Astronomy and Astrophysics, Pennsylvania State University, University Park, PA 16802; nnp@astro.psu.edu.

[3] Department of Physics, Pennsylvania State University, University Park, PA 16802.

[4] Center for Particle Astrophysics, Pennsylvania State University, University Park, PA 16802.

2. MODEL DESCRIPTION

HNe, especially the Ic types associated with GRBs but also some of the unassociated ones, are thought to be due to WR progenitors (Nomoto et al. 2008), and as such are expected to have had a strong stellar wind phase prior to the explosion. The model of a HN ejecta expanding in a stellar wind used in this Letter is based on the model of Wang et al. (2007). Thus, we consider a stellar wind environment around the progenitor which is characteristic of WR stars. Assuming a mass-loss rate $\dot{M}$ and a wind velocity v_w, the density profile of the wind is written as $\rho(r) = 5 \times 10^{11} A_* r^{-2}$ g cm^{-1}, where A_* ($\propto \dot{M}/v_w$) = 1 corresponds to $\dot{M} = 10^{-5}\ M_\odot$ yr^{-1} and $v_w = 10^3$ km s^{-1} (Wang et al. 2008).

The outer envelope regions (the ejecta) of the exploding HN, as shown by Soderberg et al. (2006), have a kinetic energy distribution $\propto (\Gamma\beta)^{-\alpha}$. In this Letter we assume $E_k = 10^{52}(\Gamma\beta/0.1)^{-2}$ ergs, where the velocity of the bulk of the ejecta ranges from $\Gamma\beta \simeq 0.1$ up to semirelativistic values ($\Gamma\beta \simeq 1$), where $\beta = v/c$ and Γ are the ejecta normalized velocity and bulk Lorentz factor, respectively.

For nonrelativistic ejecta ($\Gamma\beta \lesssim 0.5$, $E_k \gtrsim 4 \times 10^{50}$ ergs), the free expansion phase before deceleration sets in lasts for $440(\Gamma\beta/0.5)^{-5} A_*^{-1}$ days. Therefore, nonrelativistic ejecta cannot dissipate their kinetic energy within the 10–20 day typical timescale of the UV–optical photon radiation from HNe. Thus after the optical emission from HNe has declined, we may not expect secondary photons originating from $p\gamma$-interactions, even if a sufficient amount of high-energy protons are produced.

On the other hand, the bulk of the kinetic energy of the mildly relativistic ejecta are dissipated at a radius $R_d \simeq 10^{16}(\Gamma\beta/1.0)^{-1} A_*^{-1}$ cm. Since $\beta \simeq 1$ for such ejecta, all the mildly relativistic ejecta dissipate their kinetic energy within 10 days, as long as $A_* \gtrsim 1$. Therefore, hereafter we consider only the most energetic component $\Gamma\beta = 1$ ($E_k = 10^{50}$ ergs) of the mildly relativistic ejecta.

For the ejecta with $\Gamma\beta = 1$, the magnetic field at the dissipation radius R_d may be estimated as $B^2/8\pi = \epsilon_B \rho(R_d) c^2$, where $\epsilon_B = 0.1\epsilon_{B,-1}$ is the fraction of the equipartition value of the magnetic field. Thus, we obtain $B \simeq 3.4\epsilon_{B,-1}^{1/2} A_*^{3/2}$ G.

The maximum energy of accelerated protons for the mildly

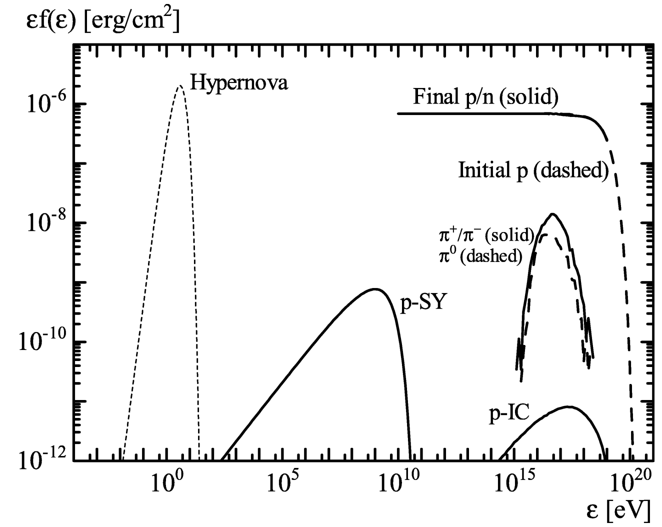

FIG. 1.—Spectra of the initial protons, and of the surviving protons/neutrons after the timescale $R_d/c = 3.3 \times 10^5$ s ~ 4 days, for a hypernova explosion in a wind characterized by the mass-loss rate $A_* = 1$. The spectra of secondary particles and photons created during this timescale are also plotted, including pions, proton synchrotron photons (labeled p-SY), and proton inverse Compton photons (labeled p-IC), not all of which can be directly observed. The fluence is normalized assuming a distance $D = 100$ Mpc. The hypernova soft photon spectrum is plotted with thin dashed lines.

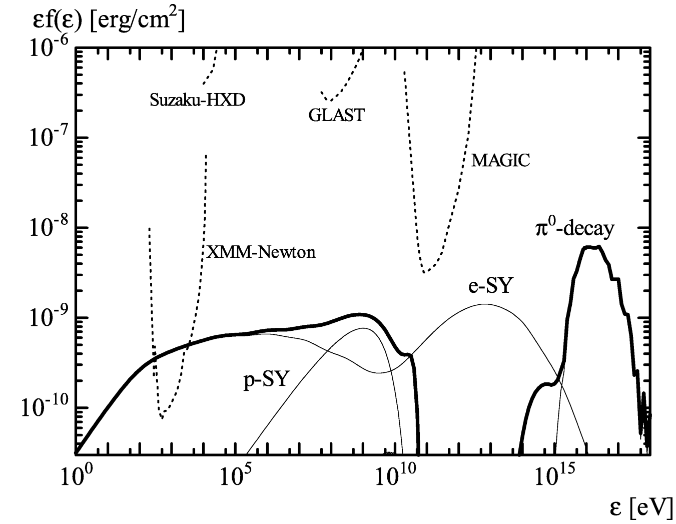

FIG. 2.—Spectral fluence of combined secondary and tertiary photons from the hypernova of Fig. 1 (*thick solid line*), at the distance $D = 100$ Mpc for $A_* = 1$, integrated over $R_d/c = 3.3 \times 10^5$ s. Thin curves denote electron/positron synchrotron (labeled e-SY), proton synchrotron (labeled p-SY), and π^0-decay components emitted inside the source. The resulting photon spectrum escaping from the source, taking into account internal $\gamma\gamma$-absorption by the hypernova soft photon field, is shown by heavier lines. The sensitivity curves for representative instruments are plotted with dotted lines. The curves for *XMM-Newton* and *Suzaku* are normalized by 100 ks integration time.

relativistic ejecta may be written as $\varepsilon_{\max} \simeq eBR$. With the above values of B and R_d, we obtain $\varepsilon_{\max} \simeq 10^{19}\epsilon_{B,-1}^{1/2}A_*^{1/2}$ eV, for the most energetic ejecta dissipated within 10 days. Adopting this value, the energy distribution of accelerated protons is assumed to be $N_p(\varepsilon_p) \propto \varepsilon_p^{-2}\exp(-\varepsilon_p/\varepsilon_{\max})$. The amount of protons is normalized by an efficiency factor 1/6 for the conversion of dissipated kinetic energy (10^{50} ergs) into energy of accelerated protons (Hillas 2005).

The usually observed low-energy (~1 eV) photons from HNe are attributed largely to radioactive decay in the nonrelativistic ($\Gamma\beta \simeq 0.1$) ejecta. After an initial rise and just after the dissipation of the ejecta (~ a few days), the changes in the optical luminosity of the HN are not very drastic (1–2 mag), as shown in Pian et al. (2006). Therefore, a constant luminosity for a few tens of days may be a reasonable approximation. As shown in Mazzali et al. (2006) the peak flux is at 4000–5500 Å, which is considered to be due to broad emission lines of several types of metals. Here we mimic this photon field by a thermal photon field with a temperature $T = 1$ eV and luminosity $L_{\rm HN} = 10^{43}$ ergs s^{-1}, which is compatible with the bolometric luminosity of SN 1998bw around its peak brightness (Galama et al. 1998).

Another source of low-energy photons is synchrotron radiation from electrons accelerated in the ejecta. For mildly relativistic shocks, the typical Lorentz factor of accelerated electrons is less than $m_p/m_e \sim 10^3$, which implies that the typical energy of synchrotron photons is $\varepsilon_\gamma \lesssim 10^{-2}$ eV for $B = 3$ G. The cooling timescale of such electrons is ~1 day, which is much shorter than the timescales we consider. Injection of accelerated electrons may continue for a few tens of days as indicated by radio observations. The most luminous radio afterglow in HNe observed ever is in SN 2003dh (Berger et al. 2003), ~10^{41} ergs s^{-1}, which may slightly enhance pion production efficiency for the highest energy protons (>10^{18} eV). Here, for simplicity, we neglect the photon emission from accelerated electrons.

In order to calculate the pion production and the subsequent cascade processes, we carry out Monte Carlo simulations using a code developed for and discussed in a series of studies of gamma-ray burst physics (Asano 2005; Asano & Nagataki 2006; Asano & Inoue 2007). We use a simple one-zone approximation, and follow during a finite time the physical processes of pion production, pion decay, muon decay, and $\gamma\gamma$ electron-positron pair creation, as well as the usual radiation processes of synchrotron (SY) and inverse Compton (IC) emission from protons, pions, muons, electrons, and positrons. We assume that the accelerated protons are injected promptly just after the energy dissipation occurs at $r = R_d$. Since the bulk motion of the postshock region is nonrelativistic, we neglect the expansion of the ejecta after that.

3. RESULTS

First, we consider a HN exploding in a standard wind with $A_* = 1$. As shown in Figure 1, even after the accelerated protons have been irradiated by the HN photons for $R_d/c \sim 4$ days, most of the protons still retain a large fraction of their energy. The pion-production timescale $t_{p\gamma}$ is inversely proportional to the HN photon density $\propto LT^{-1}R_d^{-2}$. Following Wang et al. (2007) the fraction of the energy lost by protons to pions is estimated as $f_{p\gamma} \equiv R_d/(ct_{p\gamma}) = 0.04A_*$, which is consistent with our numerical result. Charged pions of typical energy ~10^{16} eV and a total fluence of 4.5×10^{46} ergs are produced within this timescale, which give rise to electromagnetic cascades.

As shown in Figure 2, if one neglects the $\gamma\gamma$-absorption effects, a spectral bump of SY emission appears around the TeV–10 TeV energy range. This bump is due to SY photons of $15\epsilon_{B,-1}^{1/2}A_*^{3/2}$ TeV from positrons and electrons from muon decay. Since the SY photon energy scales as the square of the energy of the emitters, the photon bump energy range spreads over 2–3 orders of magnitude. The inclusion of $\gamma\gamma$-effects leads to these photons being absorbed through interaction with the HN soft photon field, creating electron-positron pairs of $(1\text{–}10)\epsilon_{B,-1}^{1/2}A_*^{3/2}$

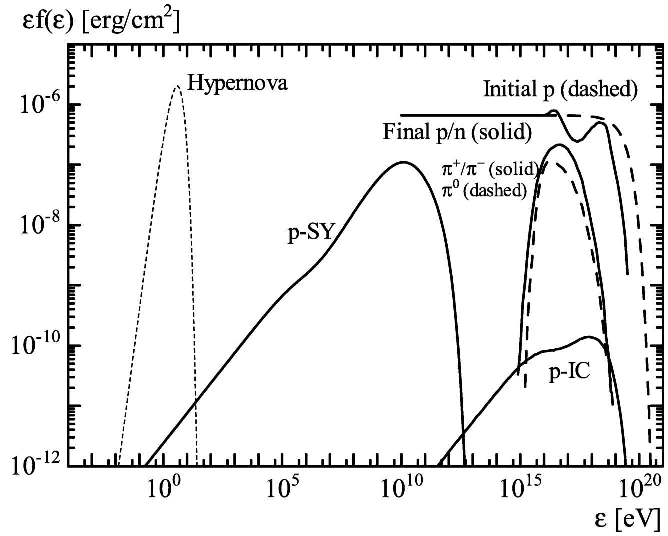

FIG. 3.—Primary and secondary particle and photon spectra, similar to Fig. 1, for a hypernova at the same distance $D = 100$ Mpc but in a denser wind environment of $A_* = 5$.

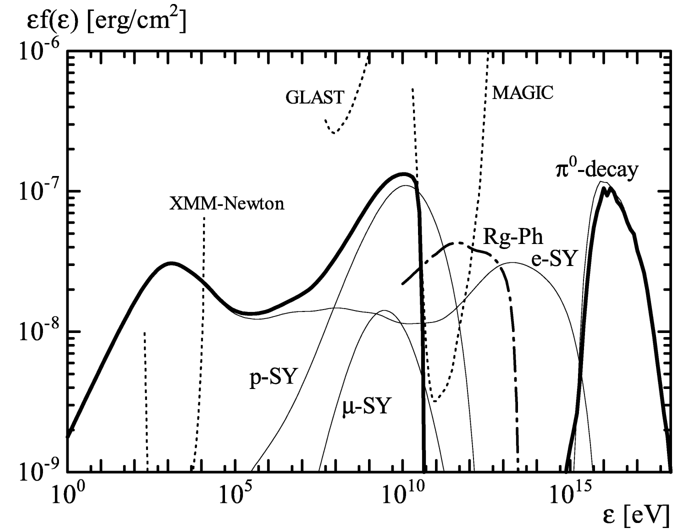

FIG. 4.—Secondary and tertiary photon spectra, similar to Fig. 2 but for the hypernova of Fig. 3 at $D = 100$ Mpc in a wind of $A_* = 5$. In addition, the muon synchrotron component (labeled μ-SY), whose typical energy is determined by a balance between the cooling timescale and lifetime (see, e.g., Asano 2005), is also plotted. The dash-dotted line is the regenerated photon spectrum due to CMB attenuation of $\sim 10^{16}$ eV photons.

TeV. The secondary pairs emit SY photons over a wide energy range (which should be twice as wide as that of the TeV bump), from a few keV to a few hundreds of keV. These pairs cool so promptly that the result is a simple power-law spectrum due to cooled pairs below 100 eV. The secondary photon emission is expected to last as long as the HN emits optical photons, even though the cooling time of the electrons that emit X-ray photons is only about 1 minute. These photons will be observed with various present-day X-ray telescopes for 100 ks integration, as shown in Figure 2, unless the X-ray afterglow emission of a GRB overwhelms it, e.g., as seen in GRB 060218/SN 2006aj.

Around the GeV region, proton SY emission yields a bump in the photon spectrum, as seen in Figure 2. The typical energy of proton SY photons is $2.4\epsilon_{B,-1}^{3/2} A_*^{5/2}$ GeV, and the ratio $t_{p\gamma}/t_{p,\rm syn}$ (where $t_{p,\rm syn}$ = SY cooling timescale) is $\sim 0.2(A_*\epsilon_{B,-1})^{3/2}$, which roughly agrees with the obtained energy fraction of proton SY to pions. For this distance the fluence is much lower than the *GLAST* detection limit. To detect 100 MeV photons with *GLAST* would require a HN at $\lesssim 6$ Mpc.

Another notable feature of Figure 2, around energies $\sim 10^{16}$ eV, is the prominent presence of photons from π^0-decay. Those photons escape without being absorbed by the ~ 1 eV thermal photon field assumed for the HN. However, the mean free path of these 10^{16} eV photons against $\gamma\gamma$-absorption by cosmic microwave background (CMB) photons is ~ 10 kpc (Aharonian et al. 2002), so that we cannot expect to detect such photons directly. The secondary electron-positron pairs generated by attenuation are very energetic, and are inverse Compton scattered by CMB photons, e.g., as discussed for GRBs (Razzaque et al. 2004; Murase et al. 2007 and references therein). These boosted photons can pair-produce again, and the process repeats itself until the energy of the degraded photons is in the 1–10 TeV range. The mean free path of these regenerated 1–10 TeV photons is longer than 100 Mpc, and they can reach the Earth. As long as the intergalactic magnetic field is weak enough, the delay time of TeV photons emitted by ~ 100 TeV electrons/positrons is negligible in comparison with the timescale a few days (Razzaque et al. 2004). We omit plotting the spectrum of the regenerated photons in Figure 2, since from $D = 100$ Mpc it will be hard to detect them; however, if a HN occurs in the Virgo Cluster ($D \sim 20$ Mpc), there would be a chance to detect these secondary TeV photons (see below).

Next, we consider a HN occurring in a denser wind with $A_* = 5$. This value is compatible with currently available data on wind mass losses suggesting $\dot{M} \lesssim$ a few $\times\ 10^{-4}\ M_\odot\ \rm yr^{-1}$, which refer to stars well before any explosion (Meynet & Maeder 2007). Physically, even larger values may be plausible, since one expects the mass loss to increase considerably as the evolution of the core rapidly approaches the final collapse, with a rapid increase in the luminosity and the envelope expansion rate.

In this case of $A_* = 5$, the ejecta will stall at $R_d \sim 2 \times 10^{15}$ cm within ~ 1 day, so that the nonrelativistic ejecta of $\Gamma\beta = 0.1$ can catch up with the decelerating ejecta about 10 days later. However, at least until the nonrelativistic ejecta has caught up, the secondary photons are largely observable.

Basically, the cooling timescale is shorter than the integration timescale (~ 4 days) assumed here, which results in a bumpy non-power-law energy distribution of the final protons (Fig. 3). The highest energy protons cool via SY ($t_{p\gamma}/t_{p,\rm syn} \sim 1$), while protons of $\lesssim 10^{18}$ eV cool via photomeson production ($f_{p\gamma} \sim 0.2$). If we take into account the radio emission from accelerated electrons, these complex feature of the proton spectrum may be weakened because of the high efficiency of pion production above 10^{18} eV.

In this case the proton SY emission becomes prominent, since the cooling timescale $\propto \epsilon_{B,-1}^{-3/2} A_*^{-7/2}$ is shorter. The secondary photon flux (see Fig. 4) is, as expected, larger than in the lower density wind (Fig. 2) case. However, even this higher density wind case gives, from $D = 100$ Mpc, an insufficient flux to be detectable with *GLAST* (see Fig. 4). However, photons from similar HNe within 40 Mpc would be detectable by *GLAST*. In addition, the regenerated TeV photons are promising targets of ACTs. In Figure 4 we plot the regenerated photon spectrum obtained by the same numerical simulation as in Murase et al. (2007). They are well above the detection limit of present-day ACTs even for $D = 100$ Mpc.

Secondary X-ray photons are emitted by electron-positron pairs originating from photons due to both proton SY and SY photons from muon-decay positrons. This is because the energy of the proton SY photons shifts higher $\propto \epsilon_{B,-1}^{3/2} A_*^{5/2}$. Since the energy range of the absorbed proton SY photons ($\sim 10^{11}$ eV) is narrow, the secondary pairs produce a characteristic peak in the fluence spectrum around $0.4\epsilon_{B,-1}^{1/2} A_*^{3/2}$ keV. These photons are indirect evidence of proton SY, and can be easily detected with present-day instruments.

4. SUMMARY AND DISCUSSION

We have shown that secondary gamma and X-rays, correlated with the initial thermal optical emission of hypernovae in the first ~ 10 days, can provide evidence for proton acceleration, as well as provide a diagnostic for amplification of magnetic field in the blast wave, and for the mass-loss rate in the progenitor stellar wind prior to the explosion. There are three main spectral components of secondary photons: (1) X-ray photons emitted by electron-positron pairs originating from $\gamma\gamma$-interactions initiated by synchrotron photons from muon-decay positrons or protons, (2) synchrotron photons emitted by protons in the GeV band, and (3) regenerated TeV photons emitted by electron-positron pairs generated by CMB attenuation of π^0-decay photons around 10^{16} eV. The X-ray photons are the most promising targets, so that follow-up observations of HNe with X-ray telescopes are indispensable to find evidence of proton acceleration. Soft SY photons from accelerated electrons may also enhance the electromagnetic cascades by interacting with photons from pion decay. The interesting π^0-decay photon signature (component 3) is also an interesting candidate for detection with ACTs in the dense-wind case ($A_* = 5$).

If a HN occurs in our Galaxy at a distance of 10 kpc (the rate for which should be $\lesssim 10^{-3}$ to 10^{-4} yr^{-1}), our results indicate an expected flux 10^{-7} to 10^{-5} ergs cm^{-2} s^{-1} at 10 GeV for $A_* = 1$–5, due to proton SY and/or secondary leptons, detectable by *GLAST*. By comparison, the most luminous "normal" SNRs observed with EGRET (Esposito et al. 1996) have fluxes of $\sim 10^{-10}$ ergs cm^{-2} s^{-1} at 10 GeV. TeV photon detections are not expected to be detectable from a Galactic HN, since the photon regeneration process mean free path is too long to be effective here. Our simulations show also that the secondary $\gtrsim$ TeV neutrinos from the cascades in a Galactic HN have a spectral peak at 10^{16} eV with a flux of 10^{-4} to 10^{-3} ergs cm^{-2}, well above the detection limit of IceCube. Thus, one would expect to detect continuous TeV neutrino emission for a few days from such Galactic HNe.

For HNe at distances $D \sim 100$ Mpc, the X-rays (component 1) will be easily detectable by *XMM*, the sub-TeV radiation is marginally detectable near the low-energy threshold by MAGIC and similar ACTs, and the GeV photons from a proton SY (component 2) are difficult to detect with *GLAST*. However, for $A_* = 5$, HNe in the Virgo cluster ($D \sim 20$ Mpc) would be easily detectable at GeV energies by *GLAST*, as would also the regenerated TeV photons. Such detections would provide constraints on HN models. For example, the duration of the proton SY emission or the X-ray spectral peak at 1 keV gives an estimate of the survival timescale of magnetic fields amplified by the nonlinear MHD turbulence excited by cosmic rays (Bell & Lucek 2001). Since the maximum proton energy is not so sensitive to ϵ_B, the spectral component 1 due to the cascades from pion production will not change drastically, even for $\epsilon_B \ll 0.1$, although the direct proton SY (component 2) can become negligible. In such cases, the disappearance of the X-ray spectral peak shown in the $A_* = 5$ case would be a diagnostic for such low ϵ_B values.

The intensity of the cascades depends on the wind density, providing a diagnostic for the progenitor mass-loss rate. For example, with $A_* = 0.2$ and other parameters as in Figure 2 the fluxes are undetectable even by X-ray instruments, unless the source is extremely near. On the other hand, larger values of $A_* \sim 10$ (e.g., as suggested by Campana et al. [2006] for SN 2006aj) would give higher fluxes than those of Figure 4, enhancing the probability of detection at $D \sim 100$ Mpc at TeV, GeV, and X-ray energies.

We thank K. Nakazawa and K. Murase for providing the sensitivity curves of various instruments, S. Razzaque and S. Inoue for valuable discussions, the referee for valuable comments, and NSF AST 0307376 for partial support.

REFERENCES

Aharonian, F. A., Timokhin, A. N., & Plyasheshnikov, A. V. 2002, A&A, 384, 834
Asano, K. 2005, ApJ, 623, 967
Asano, K., & Inoue, S. 2007, ApJ, 671, 645
Asano, K., & Nagataki, S. 2006, ApJ, 640, L9
Bell, A. R., & Lucek, S. G. 2001, MNRAS, 321, 433
Berger, E., et al. 2003, Nature, 426, 154
Budnik, R., Katz, B., MacFadyen, A., & Waxman, E. 2008, ApJ, 673, 928
Campana, S., et al. 2006, Nature, 442, 1008
Esposito, J. A., Hunter, S. D., Kanbach, G., & Sreekumar, P. 1996, ApJ, 461, 820
Gabici, S., & Aharonian, F. A. 2007, Ap&SS, 309, 465
Galama, T. J., et al. 1998, Nature, 395, 670
Hillas, A. M. 2005, J. Phys. G, 31, R95
Katz, B., & Waxman, E. 2008, J. Cosmol. Astropart. Phys, 01, 018
Kistler, M. D., & Beacom, J. F. 2006, Phys. Rev. D, 74, 3007
Mazzali, P. A., et al. 2006, Nature, 442, 1018
Meynet, G., & Maeder, A. 2007, A&A, 464, L11
Murase, K., Asano, K., & Nagataki, S. 2007, ApJ, 671, 1886
Nomoto, K., Tanaka, M., Tominaga, N., Maeda, K., & Mazzali, P. A. 2008, NewA Rev., in press (arXiv:0707.2219)
Pian, E., et al. 2006, Nature, 442, 1011
Razzaque, S., Mészáros, P., & Zhang, B. 2004, ApJ, 613, 1072
Soderberg, A. M., et al. 2006, Nature, 442, 1014
Wang, X. Y., Razzaque, S., & Mészáros, P. 2008, ApJ, in press (arXiv:0711.2065)
Wang, X. Y., Razzaque, S., Mészáros, P., & Dai, Z. G. 2007, Phys. Rev. D, 76, 083009
Woosley, S. E., & Bloom, J. S. 2006, ARA&A, 44, 507